CHAPTER 7: TRANSFORMING CHEVRON BRACE CONFIGURATION INTO A MULTI-LEVEL ECCENTRIC-CHEVRON (MLEC) BRACE

A method of upgrading the existing chevron braced steel frames has been presented here. Geometry and the material properties of the specimens were similar to those used in the previous chapter (*upgrade of chevron braced frames using additional vertical and diagonal members*). The braced frames were upgraded by introducing a new method which would provide better strength and ductility to the frame. After upgrade, the inelastic behaviour of chevron brace (*concentric or eccentric*) under cyclic loading was that of the two eccentric braces generated out of one chevron brace. The hysteresis loops and the energy diagrams indicated towards the achievement of an excellent seismic behaviour by the chevron turned multi-level eccentric chevron (*MLEC*) braces.

7.1 THEORY AND SPECIMEN CONFIGURATION

The old designed chevron braced frames having WF sections for all the members, made-up of JIS-SS41steel (*equivalent to ASTM-A36 steel*) were selected to be upgraded. Height of the building was 1.4 m and the sections of the beams, columns and braces remained individually constant for all the considered frames.

After buckling of a brace in an older chevron braced frame, various undesirable structural behaviours can be encountered. Significant beam deflection, unbalanced forces acting on the bean-brace connection, severe strength degradation and the loss of lateral load resisting capability (*remaining brace expected to resist lateral load by experiencing tension has also been found to become ineffective*) have been observed in those NCBFs. Here, the lintel bands were included in the chevron braced frames (*both concentric and eccentric*) to overcome such undesirable behaviours (*due the buckling of braces*).

These lintel bands were rigidly connected (*can also be connected using steel jacketing around the columns*). Elastic properties were as follows: density = 7850 kg/m^3; Young's modulus, E= 2.1×10^5 MPa and Poisson's ratio = 0.3. Half-cycle, combined hardening was considered. Plasticity properties and member sections were as given in Table 7.1.

Table 7.1 Material properties and member sections

Member	σ_y , σ_u (MPa)	ϵ_p	Section (values in mm)
Beam	276, 424	0.28	100×100×6×8
Column	276, 424	0.28	100×100×6×8
Brace	270, 409	0.37	50×50×6×6
Lintel band	270, 409	0.37	50×50×6×6

Note: σ_y is the yield stress, σ_u is the ultimate stress and ϵ_p is the plastic strain.

Global drift ratio (in radians, rad.) or limit (in %) is the roof displacement divided the building height. Drift range is the sum of the absolute positive and negative drift ratios in a displacement loading cycle. Incremental amplitude alternating cyclic loading was introduced by using displacement loading protocol. For single story frames, it was done by increasing the drift angle/ratio by 0.01 rad. (*0.005 rad. for two-story frames*), after every four cycles of loading with constant amplitude (shown in Figure 7.1).

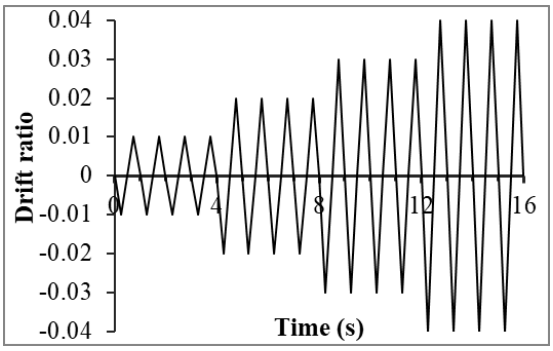

Figure 7.1 Displacement loading protocol

Increasing the size of brace to improve the lateral load capacity of the braced frames wasn't found useful in many scenarios. Inelastic buckling capacity increased by just 9.5% for 50% decrement of slenderness ratio; which would be insignificant in-front of the

theoretical elastic buckling capacity consideration of 400% increment in capacity on decrement of slenderness ratio by 50% (Roeder 1989). Slenderness of brace less than 22 was found detrimental for the tested braced frames (*under lateral cyclic loading*) as the hysteretic characteristics deteriorated considerably (Wakabayashi 1977).

Detrimental nature of very compact braces was also in the linear-perturbation, Eigen-value buckling analysis of braced frames under lateral loading. Braces having slenderness ratio smaller or equal to the frame members weren't found to appreciably increase the buckling load capacity of the braced frame under lateral loads. Rather they caused the column to buckle in some cases, which were undesirable (Narayan and Pathak 2020). Here in the present study, braces were strengthened by increasing the moment of inertia but by introducing nodes in length of the braces, to improve the buckling load capacity.

Table 7.2 Euler buckling loads (in Ton, t) under vertical load (*V*) and Lateral load (*H*)

Loading	*CBF (a, b, c)*	*EBF (a, b, c)*
V (t)	1083.6, 1361.9, 25%	917.3, 1177.8, 28%
H (t)	104.6, 189.0, 80%	100.1, 191.0, 91%

Note: 'a', 'b' and 'c' represent buckling load without lintel band, with lintel band and the improvement in load capacity (in %) respectively.

The improvement in the strength of the existing braced frames under the vertical and lateral loading by lintel band can be understood from Table 7.2. As the lintel bands have been found here to be beneficial from the strength perspective (*lateral load resisting capacity*); the remaining objective of present study was to ascertain the ductility.

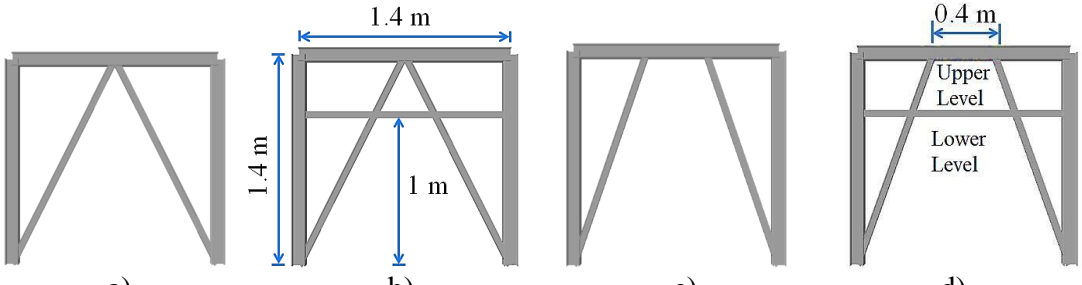

Figure 7.2 a) Old concentric chevron (*Ch*), b) Concentric chevron with lintel band (*ChLN*) c) Old eccentric chevron (*Che*) d) Eccentric chevron with lintel band (*CheLN*)

The combination of lintel band and chevron brace shown in Figure 7.2 didn't give an effect of superposition of chevron braces and the lintel bands but had its own dimension of work. The chevron brace with lintel band behaved as a new type of brace (*which was named here as a muti-level eccentric chevron, MLEC*).

7.2 EXISTING BRACED FRAME DESIGN CONSIDERATIONS

In most of the researchers, in-plane buckling of braced frame members were appreciated (*in-plane buckling of braced frames was also followed here*). According to the seismic provisions of AISC (2016), the local slenderness criteria for members in a braced frame defined by flange-width to flange-thickness ratio (b/t_f) and web-height to web-thickness ratio (h/t_w) were based on young's modulus (E) and minimum yield stress (F_y).

For moderate seismic loading, $b/t \le 0.40\sqrt{\frac{E}{R_y F_y}}$ (Equation 7.1)

For severe loading, $b/t \le 0.32\sqrt{\frac{E}{R_y F_y}}$ (Equation 7.2)

For both moderate and severe seismic loadings, $h/t \le 1.57\sqrt{\frac{E}{R_y F_y}}$ (Equation 7.3)

For global slenderness ratio (KL/r) of members was, $KL/r \le 4\sqrt{\frac{E}{F_y}}$ (Equation 7.4)

Where, 'KL' represents the effective length and 'r' represents the radius of gyration. All the members selected from experimental report followed both the local and global slenderness criteria and the discrepancies related to local damages were reduced. R_y value of 1.5 (*Maximum R_y value available in AISC-2016*) was used here for JIS-SS41 steel, which has been considered equivalent to the ASTM-A36 steel in various research works.

As a parameter, for studying the behaviour of chevron braced frames under repeated/cyclic loading, strength ratio (C) was used by Tsuji and Nishino (1988).

$$C = \frac{8.M_p.L_b}{L.L_c.A_y} \qquad \text{(Equation 7.5)}$$

Where**,** L_b, L and L_c were the lengths of brace, beam and column respectively. M_p, was fully plastic moment of beam and 'A_y' was the yield axial force of brace. They found that the beam deflected elastically for the braced frame having high C value (1.1) (*signified the capacity of beam to carry unbalanced forces)*. Large vertical displacement of beams took place in small C value (0.5, 0.8) frames and with the development of early cracks, strength was degraded considerably for the C=0.5 frame. At later stages of loading, the deformation capacity was higher in low C value frames with gentle progress of cracks.

C value of the chevron CBF considered here was 0.7. In some cases of the NCBF braced frames study, Sen *et al*. (2014, 2019) found that the chevron braced frames having weak-beams (*but, SCBF brace*) had seismic response similar to fully SCBF frames. For representing the old braced frames, weak-beams were also used here in the present study.

In the eccentric braces, provision of link length (e) to the beam length ratio, e/L less than 0.5 was found to increase the stiffness considerably (Popov 1983). In the eccentrically braced frames, the braces should be strong enough such that they remain elastic like the beams (*outside link*) and columns. Most of the plastic dissipation has to be done by links.

Popov *et al*. (1987) suggested, link length ratio, $a = \frac{e}{(M_p / V_p)} \leq 1.6$ (Equation 7.6)

The plastic shear capacity of the link, $V_p = 0.55.F_y.t_w.d$ (as per the AISC-2016 seismic provision, $Vp = 0.6.F_y.t_w.(d-2t_f)$). Where, '$d$' represented the depth of the section. Short links ($1 < a <$ or $=1.6$) undergo shear yielding; long links ($a > 2.6$), undergo flexural

yielding; and intermediate links ($1.6 < a < 2.6$) experience combination of both shear and flexural yielding (Azad et al. 2017). *e/L* value for eccentric brace used in present study was 0.3, which was less than 0.5 and the value of link length ratio, $a<1.6$. Even-then, the link segment of the chevron EBF (*without upgrade*) in the present article didn't work as expected by the codal provision. Reason for such behaviour was that the beam and brace were weaker than expected for an EBF and were involved in plastic dissipation. The upgraded EBFs as MLEC braced frames avoided such problems.

7.3 RESULTS AND DISCUSSION

The non-linear inelastic behaviour of the unmodified and the modified braced frames was given by the plastic (*energy*) dissipation (*PD*), hysteresis curves, deformed shape of the specimen at maximum stressed condition (*yield zones indicated by the dark shades*), total energy of the output set for the whole specimen (*TE*) which was equal to the total internal energy minus external work, beam deflection and the rotation of the links.

As shown in Figure 7.3, the plastic dissipation by the single-storied moment frames (*B1S1*) was not significant even after the inclusion of lintel band (*LN*). Under a quasi-static cyclic loading, total energy of the output set for the whole specimen was approximately periodic and the mean of the curve was close to zero for one-story frame (*S1*) with lintel band but not for the two-story frame.

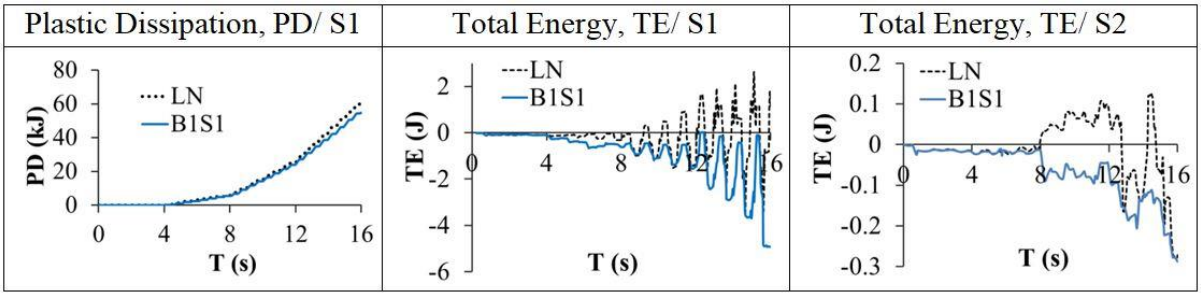

Figure 7.3 Energy curves for single story (S1) and two-story (S2) MRFs

7.3.1 Single-bay, single-story chevron CBFs

As a general trend, observed in past researches, for old designed/existing chevron braced frames (*Ch*), tension brace yielded (*in some cases, fractured without yielding due excess deflection of beam*) and the compression brace collapsed with yield hinge at the middle and end of it. Yield hinges were also observed in beam and column end connections. In most of the researches, for the chevron CBF bracing, yielding hinge was formed at the middle of the beam due to the unbalanced vertical force.

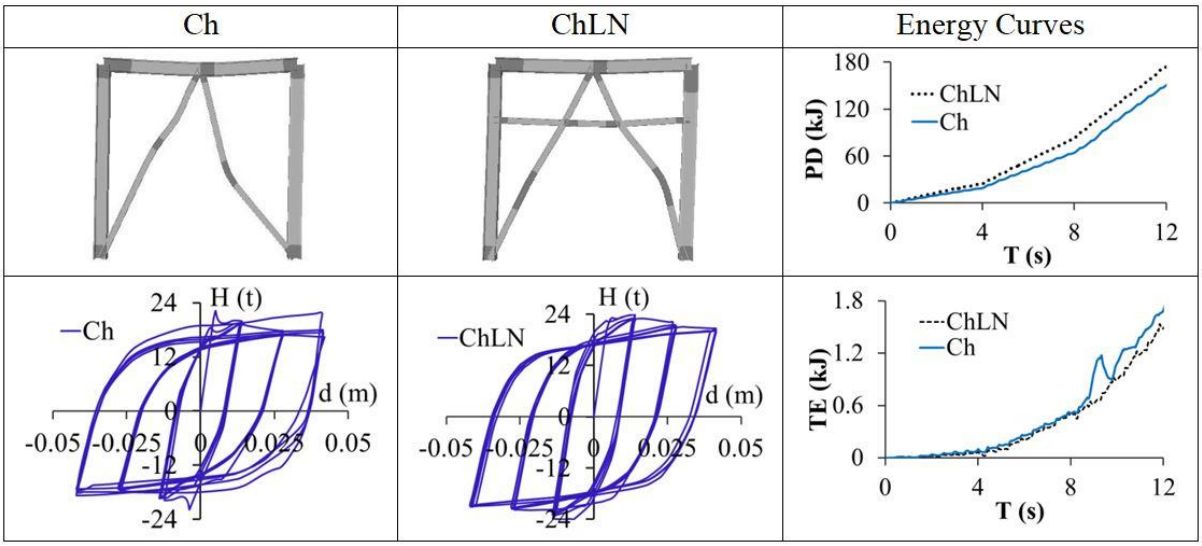

Figure 7.4 Behaviour of old concentrically braced frame and its updated multi-level counterpart (Dark part in deformed specimen shows inelastic region)

After observing the general behaviour of chevron braced frame (*i.e., the buckling of one brace in compression and tension yielding of other braces*), at 9.2 sec (*10th cycle*), the north brace buckled at a location close to upper one-third portion of its length (shown in Figure 7.4). After this, in the unloading state, the other brace experienced excessive compression and the beam experienced excessive vertical deflection.

Before the excessive compressive force on the brace could be relieved, the other brace experienced compression and inelastic deformation close to one-third point of its length (*ineffective in tension*). With considerable beam deflection and compression in both the braces, braces were not expected remain effective above 3% drift ratio (*6% drift range*).

On addition of lintel band in chevron CBF (*ChLN*), the energy dissipation capacity improved, hysteretic characteristics improved and the beam deflection reduced (see Figure 7.4). Upper part of the multi-level eccentric brace generated from the combination of chevron CBF and the lintel band didn't undergo buckling; as in that part, the length of the braces was very small. Buckling was only observed in the lower part of it. Yield hinges were also observed in beam and column end connections. Inelastic activity in beam contributed little to the energy dissipation but the contribution of the overall frame-action was throughout the loading process. The braces, lintel and its link part contributed significantly to the energy dissipation.

7.3.2 Single-bay, single-story chevron EBFs

It's a pre-requisite of chevron EBFs that the braces remain in elastic state. But, without upgrade (*Che*), starting from 1% drift limit, the braces were involved in the plastic energy dissipation. Considerable beam yielding was observed in/after the 6^{th} cycle (5.2 sec). Inelastic activity in the link contributed little to the energy dissipation and no inelastic activity was observed in it after 6^{th} cycle. At various times, excessive yielding of beam didn't allowed relief of compressive load and both braces were under excessive compression like as experienced in the CBFs (see Figure 7.5).

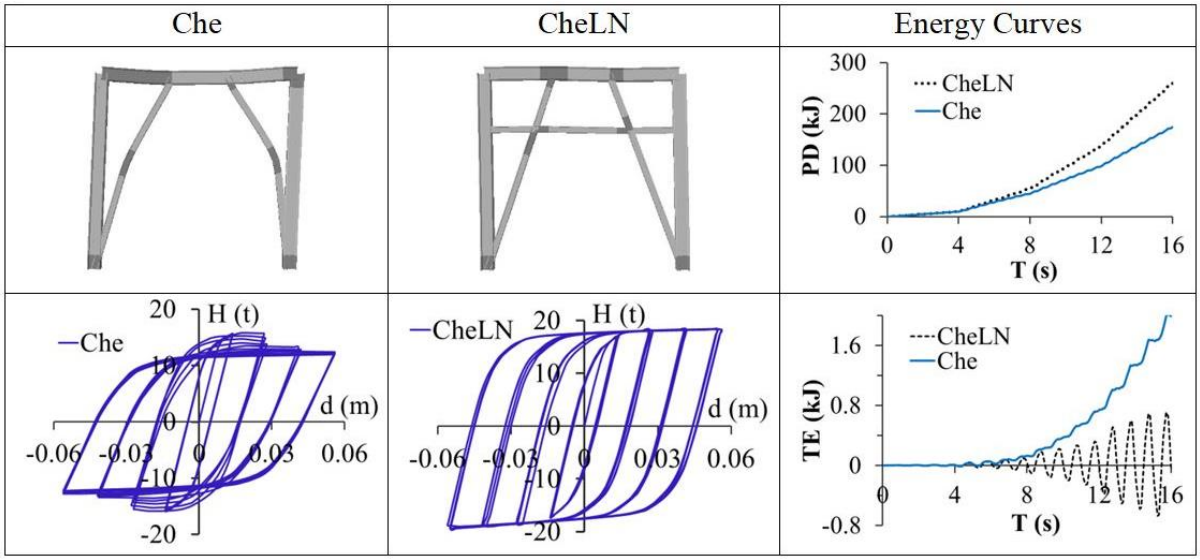

Figure 7.5 Behaviour of old eccentrically braced frame and its updated multi-level chevron counterpart

On addition of lintel band in chevron EBF (*CheLN*), an eccentric brace, which was not working as desired, was transformed into a MLEC configuration, dissipating sufficient amount of energy, having a stable hysteresis loops and good deformation capacity. Link rotation (*for both, floor beam connected link and the link part of the lintel band*) was the main source of plastic dissipation. Beam yielding was also observed due to link rotation; only at connected link. Braces yielded only at the connection ends. No yielding of column occurred at any stage (*except at the fixed base*). This multi-level brace would provide high deformation capacity (*unlike the BRBs*) and would provide the seismic behaviour as good as the BRBs, as can be deducted from the obtained hysteresis loops shown in Figure 7.5.

7.3.3 Single-bay, two-story chevron CBFs and EBFs

Good thing about the upgrade of the two-story chevron CBF/EBFs into MLEC braced frames was that the maximum contribution to the plastic dissipation was done by the braces and lintel bands with minimal contribution by the columns or the connections. Hysteresis loops (refer Figure 7.6) were similar to that of the one-story braced frames.

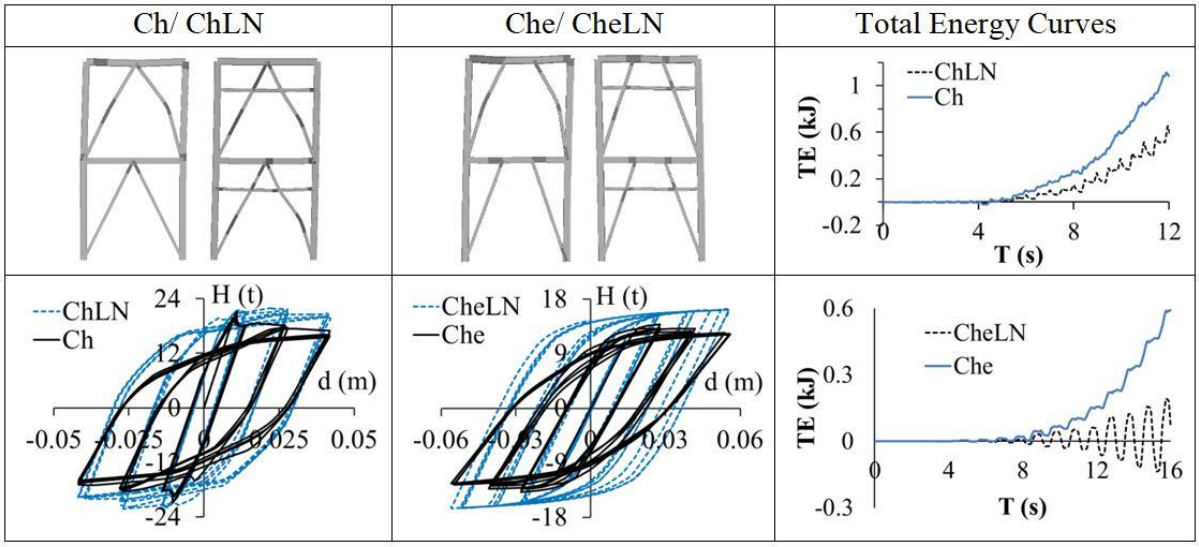

Figure 7.6 Behaviour of old eccentrically braced frame and its updated multi-level counterpart for two-story frames

As observed in the experiment studies of the two-story chevron CBF (Wakabayashi 1967) and in numerical simulations of three-story chevron CBF (Sabelli 2001), at the later stages of loading, the maximum beam deflection in chevron CBF was observed in the roof beam. Inelastic activity in the first-story brace diminished as the inelastic activity in the second story increased with the increment in the displacement amplitude. Buckling of brace was not observed in the first story. Except the second story columns yielding at the connection ends, no inelastic activity was observed in the columns. The braced frame was expected to collapse due to excessive strain concentration in the second story braces.

On addition of lintel band in the chevron CBF (*ChLN*), the energy dissipation was mostly contributed by the inelastic activity of lower part of it (*acting like eccentric braces*) and little contribution was done by the beams. Initially, the contribution of brace of the second story in plastic dissipation was higher but at later stages of loading, maximum inelastic activity was observed in the first story. Roof beam remained in elastic state throughout the loading process and yielding in the first story floor beam occurred only after the considered limit of drift range of 3%.

In the chevron EBF (*without modification, Che*), beam yielding with excessive vertical deflection in the roof beam was observed. Beam yielding at first story level was also observed at the beam-link connection ends. At later stage of loading, braces in second story experienced excessive compression (*ineffective tension*) but braces in first story entered inelastic state only at the connection ends.

On addition of the lintel band in chevron EBF (*CheLN*), major contribution to plastic dissipation was done by link rotation (*including the link part of the lintel band*). At the first story level, beam yielded only at the link end connections. In second story, the link and the beam (*at the connection end of link*) yielded due to link rotation. Columns, beams (*except at the link connection*), braces (*except at connections*) maintained the elastic state. This multi-level bracing configuration was found to limit the excess lateral deflection and provide significant deformation capacity.

7.3.4 Hysteretic behaviour

For both one and two-story braced frames, the hysteresis curves of MLEC braced frames obtained after upgrading chevron CBFs (*ChLN*) were stable and the sudden sharp peaks, as mostly observed in case of chevron CBFs (*Ch*) were minimised. The hysteresis curves of MLEC braces generated from the chevron EBFs (*CheLN*) were stable and the deterioration of the strength as observed in eccentric chevron braced frames without modification (*Che*) was not observed.

7.3.5 Deformation pattern

Referring Figure 7.7 for the CBF case, the ratio of maximum beam deflection (*B*) to the beam length observed for one-story chevron CBF (*Ch S1*) was 3% which was reduced to 1.5% on addition of lintel band (*ChLN S1*). After 9th cycle of loading, beam deflection was abrupt for '*Ch S1*' (*not that abrupt after the inclusion of lintel band*). Ratio of the

maximum beam deflection to the beam length observed for two-story chevron CBF was 1.7% in roof beam/ second-story (*Ch S22*); which was reduced to a maximum of 0.4% in first-story floor beam on addition of the lintel band (*ChLN S21*).

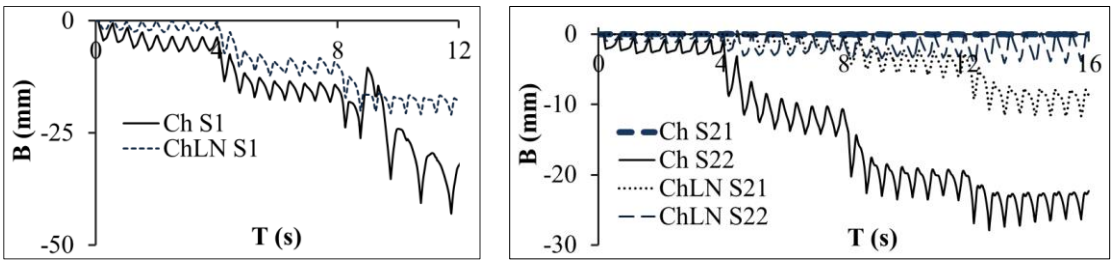

a) Single-story braced frame b) Two-strory braced frame

Figure 7.7 Floor beam deflections for chevron CBFs

First story floor-beams in both, two-story chevron CBF (*Ch S21*) and EBF (*Che S21*) had negligible beam deflection (refer Figure 7.7, Figure 7.8). For one-story chevron EBF (*Che S1*), the maximum beam deflection to the beam length ratio was 2%. On addition of lintel band (*CheLN S1*), inelastic action because of the link rotation was prominent. For two-story chevron EBF, maximum beam deflection to the beam length was 1.9% (*Che S22*) and on addition of lintel band, inelastic action because of the link rotation was prominent.

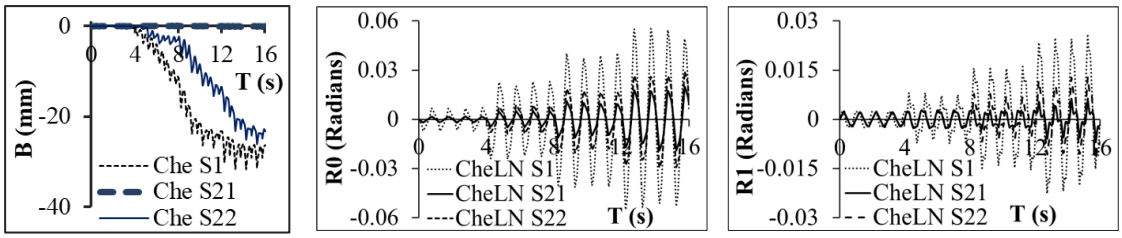

a) Beam deflection b) Beam-connected link rotation c) Lintel-band link rotation

Figure 7.8 Floor beam deflection and link rotation in chevron EBFs

For one-story EBF with lintel band (*CheLN S1*), the maximum rotation of the link connected with beam (*R0*) was 0.06 radian (rad.) and for the link part of the lintel band (*R1*), it was 0.025 rad. (refer Figure 7.8). For two-story EBF with lintel band, the maximum rotation of the link connected with beam in first story (*S21*) was 0.02 radians

and in second story (*S22*), it was 0.03 radians. For the link part in lintel band, in first story (*S21*) maximum rotation was 0.007 radians and in second story (*S22*), it was 0.01 radians.

For the link rotations, periodic curves having same period of cycle (*for one-storied frame and for both the stories of two-storied frame*) were obtained individually for the beam-link and the lintel-band connected link. Little phase difference in rotation curve was observed only for the link part available in the lintel band present in the first story of the two-storied frame (*CheLN S21*). All other curves for the link-rotation were quite uniform (*for both one and two-storied frames*) such that, if required, a periodic function with variable amplitude could be defined easily.

7.3.6 Plastic dissipation and total output energy

Maximum plastic dissipation energy up-to 12 seconds (*displacement protocol shown in Figure 7.1*) for two-story concentric CBF without and with lintel band was 96 and 131 kJ respectively (*151 and 174 kJ for one-story CBF*). Up-to 16 seconds, for two-story EBF without and with lintel band, plastic dissipation was 100 and 138 kJ respectively (*174 and 260 kJ for single-story EBF*). For braced frames which were able to provide stable and balanced Hysteresis loops (*both one and two-story, MLEC braced frames generated from chevron EBFs*), periodic curves of total output energy (TE) were obtained and the mean of these TE curve was found to be equal to zero. Since, the MLEC braced frames providing such outputs had higher strength than their old designed counterparts, such pattern of TE curves can be considered here as a parameter of both the strength and the stability of the balanced hysteresis loops.

7.4 CONCLUDING REMARKS

The EBFs and CBFs were upgraded by adding lintel bands in them (*resulting into multi-level eccentric chevron braced frame configurations for both the EBFs and the CBFs*). The eccentrically braced frames were upgraded to a very good extent (*lateral load resistance was improved, hysteresis curves were both stable and balanced, energy dissipation was mostly done by the links*).

The structural behaviour of the CBFs were also improved significantly and even initial buckling peaks (*observed in the hysteresis curves of the unmodified CBF*) were also eradicated to a considerable extent but the strength degradation at the later stages of loading was still observed. Conclusions have been discussed elaborately in the last chapter, 'SUMMARY AND CONCLUSIONS'.